

RESEARCH ARTICLE

# Heterogeneous Ag-TiO<sub>2</sub>-SiO<sub>2</sub> composite materials as novel catalytic systems for selective epoxidation of cyclohexene by H<sub>2</sub>O<sub>2</sub>

Xin Wang<sup>1,2\*</sup>, Jianyue Xue<sup>1,2</sup>, Xinyun Wang<sup>1,2</sup>, Xiaoheng Liu<sup>3</sup>

**1** College of Chemistry and Materials Engineering, Chaohu University, Chaohu, Anhui, China, **2** Institute of Novel Functional Materials and Fine Chemicals, Chaohu University, Chaohu, Anhui, China, **3** Key Laboratory of Soft Chemistry and Functional Materials of the Ministry of Education, Nanjing University of Science and Technology, Nanjing, Jiangsu, China

\* [wangxin@chu.edu.cn](mailto:wangxin@chu.edu.cn)



## Abstract

TiO<sub>2</sub>-SiO<sub>2</sub> composites were synthesized using cetyl trimethyl ammonium bromide (CTAB) as the structure directing template. Self-assembly hexadecyltrimethyl- ammonium bromide TiO<sub>2</sub>-SiO<sub>2</sub>/(CTAB) were soaked into silver nitrate (AgNO<sub>3</sub>) aqueous solution. The Ag-TiO<sub>2</sub>-SiO<sub>2</sub>(Ag-TS) composite were prepared via a precipitation of AgBr in soaking process and its decomposition at calcination stage. Structural characterization of the materials was carried out by various techniques including X-ray diffraction (XRD), scanning electron microscopy (SEM), transmission electron microscopy (TEM), N<sub>2</sub> adsorption-desorption and ultraviolet visible spectroscopy (UV-Vis). Characterization results revealed that Ag particles were incorporated into hierarchical TiO<sub>2</sub>-SiO<sub>2</sub> without significantly affecting the structures of the supports. Further heating-treatment at 723 K was more favorable for enhancing the stability of the Ag-TS composite. The cyclohexene oxide was the major product in the epoxidation using H<sub>2</sub>O<sub>2</sub> as the oxidant over the Ag-TS catalysts. Besides, the optimum catalytic activity and stability of Ag-TS catalysts were obtained under operational conditions of calcined at 723 K for 2 h, reaction time of 120 min, reaction temperature of 353 K, catalyst amount of 80 mg, aqueous H<sub>2</sub>O<sub>2</sub> (30 wt.%) as oxidant and chloroform as solvent. High catalytic activity with conversion rate up to 99.2% of cyclohexene oxide could be obtainable in water-bathing. The catalyst was found to be stable and could be reused three times without significant loss of catalytic activity under the optimized reaction conditions.

## OPEN ACCESS

**Citation:** Wang X, Xue J, Wang X, Liu X (2017) Heterogeneous Ag-TiO<sub>2</sub>-SiO<sub>2</sub> composite materials as novel catalytic systems for selective epoxidation of cyclohexene by H<sub>2</sub>O<sub>2</sub>. PLoS ONE 12(5): e0176332. <https://doi.org/10.1371/journal.pone.0176332>

**Editor:** Elena A. Rozhkova, Argonne National Laboratory, UNITED STATES

**Received:** November 27, 2016

**Accepted:** April 10, 2017

**Published:** May 11, 2017

**Copyright:** ©2017 Wang et al. This is an open access article distributed under the terms of the [Creative Commons Attribution License](https://creativecommons.org/licenses/by/4.0/), which permits unrestricted use, distribution, and reproduction in any medium, provided the original author and source are credited.

**Data Availability Statement:** All relevant data are within the paper and its Supporting Information files.

**Funding:** This work was supported by the Natural Science Foundation of Anhui Province (No. KJ2013B161) to XW, the Special Project of the Scientific Research Institute Foundation (No. XLY-201319) to XW and the Dr. Scientific Research Foundation of Chaohu University to XW. The funders had no role in study design, data collection

## Introduction

The direct oxidation of hydrocarbons is a field of academic and industrial importance [1,2]. From an industrial point of view, epoxides are largely used for the synthesis of perfume materials, anthelmintic preparations, epoxy resins, plasticizers, drugs, sweeteners, etc [3]. Selective oxidation of olefins to epoxides is a pivotal reaction in trade mark of fine chemical synthesis [4]. The oxidants for the epoxidation of alkenes include peracids, organic peroxides, hydrogen peroxide, and molecular oxygen [5]. Epoxidation reactions of alkenes generally require the

and analysis, decision to publish, or preparation of the manuscript.

**Competing interests:** The authors have declared that no competing interests exist.

presence of a catalyst. Compared with homogeneous catalysts, heterogeneous catalysts have many advantages such as easy separation and facile recovery of the solid catalyst from the reaction mixture for recycling without tedious work up [6]. Heterogeneous catalytic systems are better than similar homogenous catalytic systems in terms of separation of reaction products from the catalyst [7,8]. Up to now, transition metals or rare earth modified metal oxides have been studied widely [9,10]. Noble metals (such as Ag) have also received extensive attention due to their important potential applications [11,12]. However, noble metal modified composite oxide on the special interface have rarely been investigated. Therefore, the epoxidation of alkene derivatives using Ag as heterogeneous catalyst has been studied [13]. Cyclohexene oxide and its epoxide are important intermediate in organic process industry, and can be made by epoxidation of cyclohexene [14,15]. Therefore the catalytic epoxidation of cyclohexene remains challenging in industry. The catalytic epoxidation using metal oxides as catalysts with high selectivity under mild reaction conditions has become an important researching field [16,17]. The development of catalysts that may operate at room temperature and pressure for the transformation of relatively cheap and available substrates into valuable functionalized products has attracted the attention from both academy and industry [18]. Recently, many researchers have designed a series of strategies to load noble metal (Ag) for the catalytic reaction [19–21].

In this work, Ag-TS composite were prepared through a self-assembly process by soaking TiO<sub>2</sub>-SiO<sub>2</sub> in AgNO<sub>3</sub> aqueous, and the influence of catalytic activity of Ag-TS composite were also discussed. Their catalytic performances for the oxidation of cyclohexene using H<sub>2</sub>O<sub>2</sub> as oxidant were studied, and the effects of Ag content in the catalysts were investigated. Compared with the above reported methods, this process does not need any additional reagents. The calcined composite materials were used as the catalyst for the epoxidation of cyclohexene.

## Materials and methods

### Preparation of Ag-TiO<sub>2</sub>-SiO<sub>2</sub> composite

All the chemicals were obtained from Nanjing Chemical Reagents and used without further purification. Deionized water was used in all sample preparation. Titanium(IV)n-butoxide (0.7 g) and TEOS(0.5g) were added dropwise to a TEA (6.5 g) solution. The mixture was stirred for 25 min at 298 K until a pale yellow solution was obtained, which was then transferred to a sample trough. Toward this, 0.15 g of gelatin was dissolved in 23 g of deionized water and 0.6 g of CTAB with stirring at 303 K. The sample though was sealed and left undisturbed at 293–297 K for 48 h until a film to present on its air-water interface. The film was transferred to a glass substrate, washed by deionized water to remove excess CTAB, and then soaked in a silver nitrate (AgNO<sub>3</sub>) aqueous solution of 0.05 mol·L<sup>-1</sup> for 48 h. Finally, the soaked film was heated in a muffle at different temperature for 2 h.

### Characterizations

The X-ray diffraction patterns of samples were obtained at Rigaku D/max2500 X-ray diffractometer (XRD) using Cu K $\alpha$  radiation ( $\lambda = 0.154$  nm). Scanning electron microscope (SEM) of JEOL-6380 LV and energy dispersive spectrometer (EDS) with EDAX Genesis 2000 were applied to determine the morphologies and compositions. The morphologies were further identified with a JEOL JEM-2100 transmission electron microscope (TEM) at 200 kV coupled with a Gatan794 charge coupled device (CCD) camera, N<sub>2</sub> adsorption-desorption measurements were performed on a Micromeritics ASAP 2020 apparatus. All samples were ultrasonically dispersed in water and dried over a copper grid. The ultraviolet visible (UV-Vis) spectra

were recorded on a Beijing Persee UV-T9CS spectrometer in the wavelength range of 300–600 nm at room temperature.

## Epoxidation of cyclohexene

The catalytic performance of Ag-TS composite for the epoxidation of cyclohexene was investigated in a 100 mL erlenmeyer flask equipped with a stirrer, thermometer, and reflux condenser. In a typical batch experiment, to a flask containing 80 mg of catalyst, 12 mL of chloroform and 6 mL of 30% mass fraction H<sub>2</sub>O<sub>2</sub> were added into the flask. Subsequently, cyclohexene (6 mL) was added and the contents of the flask were kept in the water bath on a magnetic hot plate for 120 min with continuous stirring at 353 K. After reaction for 2 h, the catalyst was separated from the reaction solution by centrifugation. Then this separated catalyst was dried at 353 K overnight and calcined in air at 723 K for 120 min, to obtain the regenerated catalyst. The catalytic performance of the regenerated catalyst was investigated as the same procedure as the fresh catalyst. The concentrations in the solution was analyzed by High Performance Liquid Chromatography (HPLC) of DIONEX U-3000 with an ultraviolet detector of VWD-3100. The chromatographic conditions were as following: 0.02 mol·L<sup>-1</sup> methanol aqueous solution was used as mobile phase, the flow rate was set at 1.0 mL·min<sup>-1</sup>, the wavelength of UV irradiation was 210 nm, the column temperature was 298 K and the injection volume was 10 μL. The epoxide yield, the selectivity, the conversion of cyclohexene oxide and the selectivity to by-products were evaluated using Eqs (1–4):

$$\text{Epoxide yield} = (n_{\text{epoxide}}/n_{\text{cyclo-C}_6\text{H}_{10},\text{introduced}}) \times 100 \quad (1)$$

$$\text{Selectivity to epoxide} = (n_{\text{epoxide}}/n_{\text{cyclo-C}_6\text{H}_{10},\text{introduced}} - n_{\text{cyclo-C}_6\text{H}_{10},\text{unreacted}}) \times 100 \quad (2)$$

$$\begin{aligned} \text{Conversion of cyclo - C}_6\text{H}_{10} \\ = (n_{\text{cyclo-C}_6\text{H}_{10},\text{introduced}} - n_{\text{cyclo-C}_6\text{H}_{10},\text{unreacted}})/n_{\text{cyclo-C}_6\text{H}_{10},\text{introduced}} \times 100 \end{aligned} \quad (3)$$

$$\text{Selectivity to by - products} = n_{\text{by-product},i}/(n_{\text{cyclo-C}_6\text{H}_{10},\text{introduced}} - n_{\text{cyclo-C}_6\text{H}_{10},\text{unreacted}}) \times 100 \quad (4)$$

## Results and discussion

### Morphology and structure

The XRD pattern of the four uncalcined materials are displayed in Fig 1 (a:Ag-SiO<sub>2</sub>; b:Ag-TiO<sub>2</sub>; c:TiO<sub>2</sub>-SiO<sub>2</sub>; d:Ag-TiO<sub>2</sub>-SiO<sub>2</sub>). A predominant peak could be observed with four samples in the 2θ range from 2° to 8°. This obvious reflection appeared at small angle region which implied ordered structures inside of the self-assembled inorganic-organic metal oxide [22,23]. This suggests that as-prepared TiO<sub>2</sub>-SiO<sub>2</sub> materials are amorphous product. Moreover, the *d* value corresponded to the strongest peak meant for the spacing between the ordered lamellas or the diameter of the ordered mesopores inside the synthesized composite materials. The predominant peak of TiO<sub>2</sub>-SiO<sub>2</sub> (c) at 2θ = 3.75° give a *d* value of 2.39 nm. Comparison, the diffraction peak of TiO<sub>2</sub>-SiO<sub>2</sub> product is much weaker than that of Ag-doped different materials and it is obvious that the 2θ angles of Ag-doped products moved toward the smaller values, indicating the increased layer-layer or pore-pore correlation distance with an increase of Ag content.

The large-angle XRD patterns of the Ag-TS materials before and after calcination at different temperature are displayed in Fig 2. Those samples obtain the same diffraction peaks,

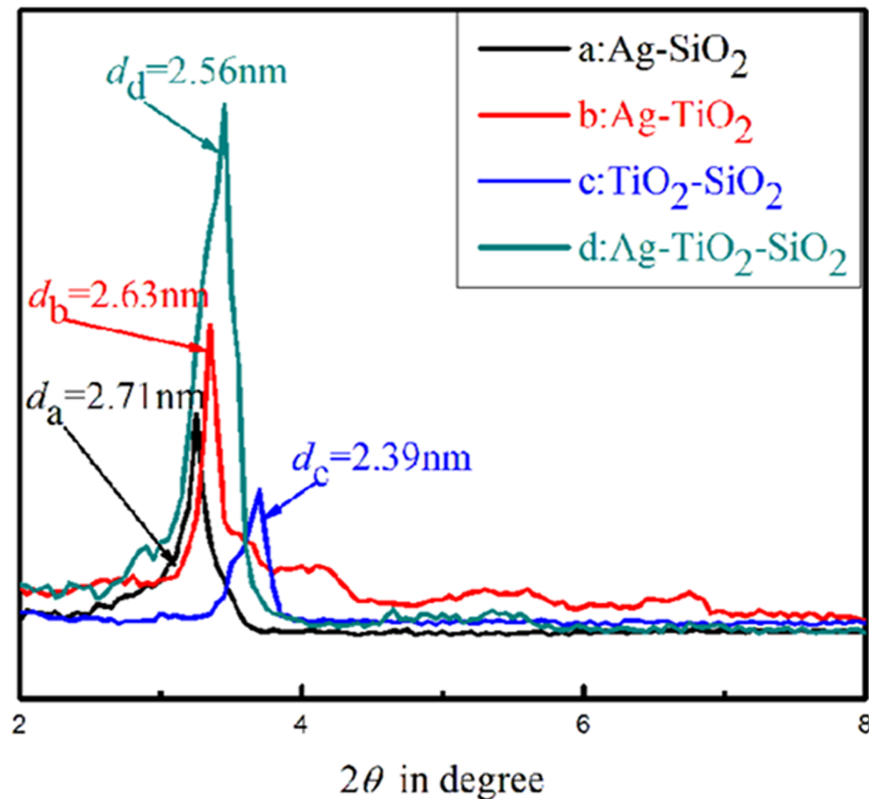


**Fig 1. LAXRD patterns of TiO<sub>2</sub>-SiO<sub>2</sub> and Ag-TiO<sub>2</sub>-SiO<sub>2</sub>.**

<https://doi.org/10.1371/journal.pone.0176332.g001>

indicates that these samples contain the same chemical composition. These peaks observed at  $2\theta$  values of 38.3, 44.2, 64.5 and 77.4° are assigned to (111), (200), (220) and (311) lattice planes of fcc metallic Ag (JCPDS Card NO. 04-0784), respectively. The lattice parameter calculated from the XRD pattern is 0.4078 nm, in agreement with the literature report [24]. It can be seen that the diffraction peaks (d) is very strong, indication of good crystallinity of the Ag-TS composite grain after calcination at 723 K. It shows that calcination does not change the crystalline phase of the Ag particles. The Ag-doped to the TiO<sub>2</sub>-SiO<sub>2</sub> particles is characteristic crystalline form,  $2\theta$  values of the major peaks locate in the range from 15° to 80° in accordance with the characteristic diffraction of Ag verifying.

The SEM micrographs coupled with Energy Disperse Spectroscopy (EDS) analysis are shown in Fig 3. This shows the SEM image(a) and EDS spectrum(b) of the Ag-TS materials calcinated at 723 K. The SEM image in Fig 3A shows the Ag-TS composite have particle diameter ranging from 300 nm to 500 nm and the surface of the particles is rough. They are composed of many small spherical aggregations. The EDS spectrum confirms the presence of Ag, Ti, Si and O in the composite, and the rest could be identified as C, N and Pt that originated from the tape and sputtering source. The Pt signals come from the plated element.

For the sake of comparison, TEM images(Fig 4) of the three different product are examined. Fig 4A shows that the granularity of spherical TiO<sub>2</sub>-SiO<sub>2</sub> particles spread at interlayer spacing of 300–600 nm. The appearance of TiO<sub>2</sub>-SiO<sub>2</sub> in the inset TEM image in Fig 4A indicates the formation of structure, the hierarchical structure of the TiO<sub>2</sub>-SiO<sub>2</sub> particles is consistent with the XRD results. It can be seen that all the Ag particles have similar spherical form in Fig 4B. The Ag particles have a range of 30–40 nm with broad size distribution. Fig 4C shows



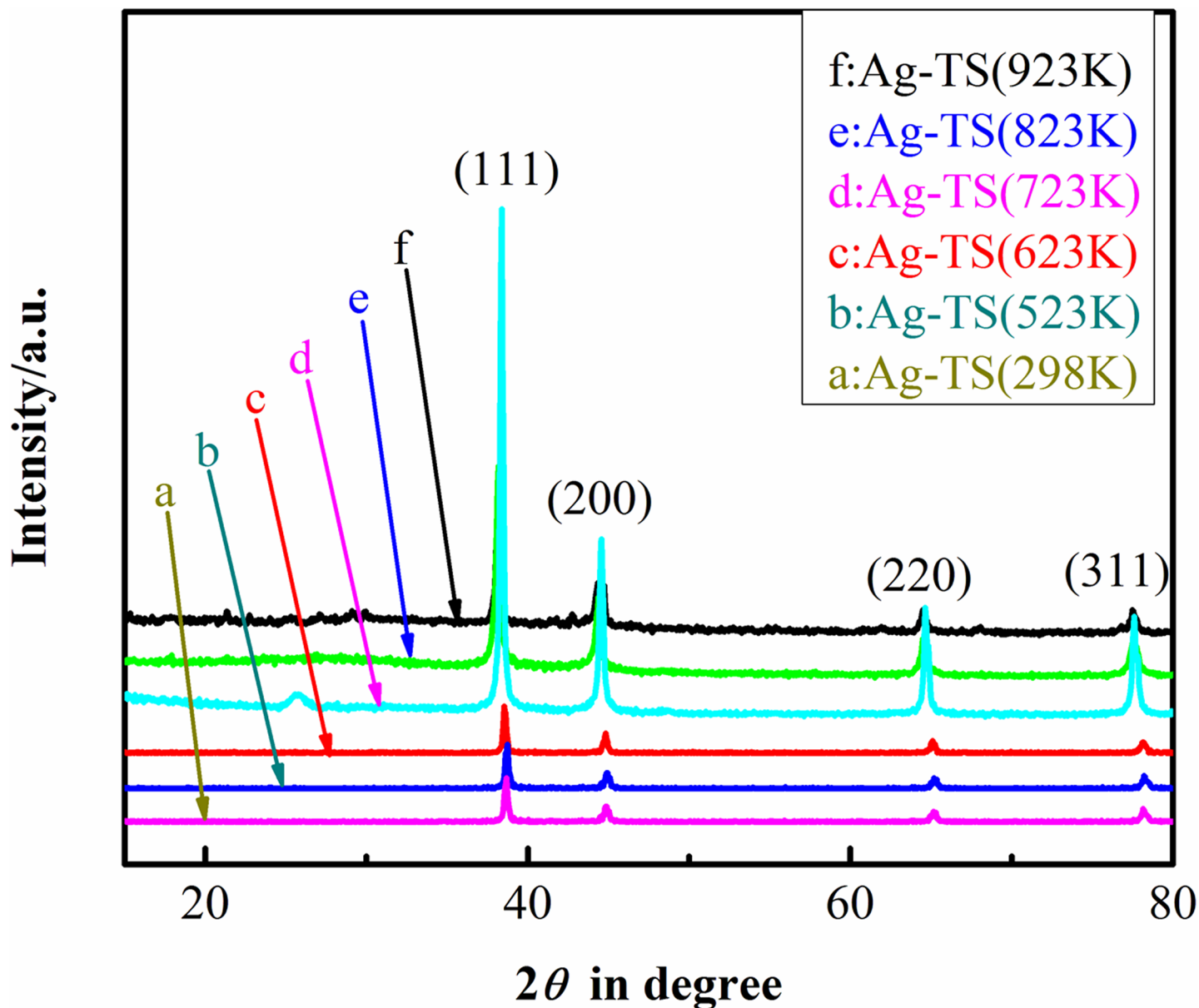


**Fig 2.** HAXRD patterns of Ag-TS composite before and after calcination at different temperature.

<https://doi.org/10.1371/journal.pone.0176332.g002>

the Ag particles attached to surface of TiO<sub>2</sub>-SiO<sub>2</sub> particles tend to grow 50–60 nm and the shape of Ag-TS particles appeared conglomerated. The Ag particles linked to TiO<sub>2</sub>-SiO<sub>2</sub> are unambiguously, further reveals the composite materials of the structure. High resolution TEM image (Fig 4D) further confirms the presence of crystalline Ag nanodomains with a lattice spacing of 0.4 nm on the products. This clearly demonstrates that Ag particles were formed and firmly doped on the TiO<sub>2</sub>-SiO<sub>2</sub> particles.

The specific surface area of Ag-TS composite can be determined by the N<sub>2</sub> adsorption-desorption measurements. In Fig 5, Ag-TS displays a type IV adsorption-desorption isotherms for mesoporous structure according to the IUPAC classification [25]. Furthermore, the type H4 hysteresis loop suggests that the slit-like mesopores formed by the Ag-TS agglomerate,

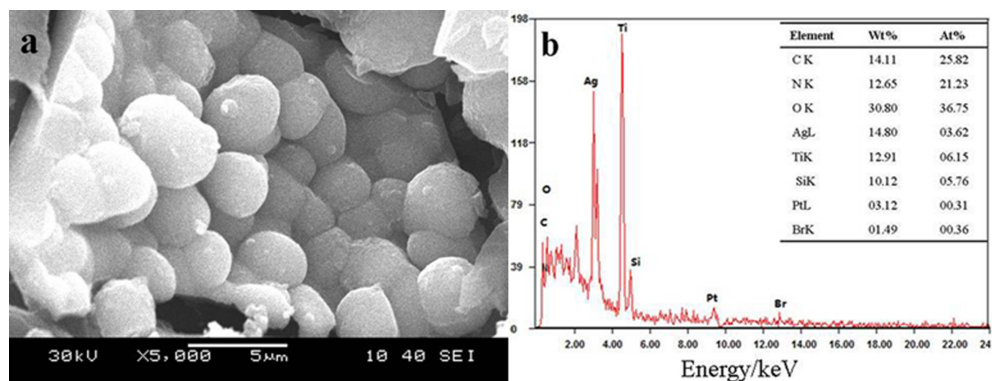


**Fig 3.** SEM image and EDS spectra of Ag-TS composite after calcination at 723K.

<https://doi.org/10.1371/journal.pone.0176332.g003>

which is in line with the TEM observation (Fig 4C). The Brunauer-Emmett-Teller (BET) surface area and pore volume are 918.9 m<sup>2</sup>·g<sup>-1</sup> and 0.57 cm<sup>3</sup>·g<sup>-1</sup>, respectively, based on the desorption branch.

The UV-Vis spectra of both pristine and calcined Ag-TS composite are presented in Fig 6. TiO<sub>2</sub>-SiO<sub>2</sub> do not show any UV visible absorption in the visible range. No absorption in the visible range for both samples could be observed while there is a strong absorption for Ag particles at  $\lambda$  of 390–430 nm. Compared with uncalcined sample with surface plasmon resonance peak at 395 nm, the same peak of calcined sample is red-shifted to 430 nm and broadened. The shift can be interpreted as the result of nano-size effect [26].

### Formation mechanism

The proposed formation mechanism of Ag-TS composite is illustrated in Fig 7. Initially, several CTAB molecules form a spherical micelle [27], the TiO<sub>2</sub>-SiO<sub>2</sub> particles with negative charges interact with the positively charged CTAB micelle through electrostatic interactions. This template plays a key role in the subsequent assembling processes [28]. When TiO<sub>2</sub>-SiO<sub>2</sub> particles formed on the air-water interfacial are soaked into the AgNO<sub>3</sub> aqueous solution, the AgBr-TiO<sub>2</sub>-SiO<sub>2</sub> composite are formed due to the precipitation of AgBr at the surfaces and voids of TiO<sub>2</sub>-SiO<sub>2</sub> particles. The AgBr-TS particles can be prepared by a reaction of Ag ions and Br ions from CTAB. Then AgBr decomposes into elemental Ag particles under visible light irradiation. The surfactant (CTAB) is destructed and it has formed a stable structure of composite particles during the calcination process. Part of the Ag particles are attached to the surface, and the rest particles remain in the interior of the TS particles.

### Epoxidation of cyclohexene

It is generally accepted that the first step in the epoxidation by the Ag-TiO<sub>2</sub>-SiO<sub>2</sub>/H<sub>2</sub>O<sub>2</sub> system is the formation of the hydroperoxo species, which are Ag particles here. The epoxidation mechanism of cyclohexene over calcined Ag-TS composite is briefly depicted in Fig 8. The catalytic reaction is similar to that occurred over TS-1 zeolite [29]. Firstly, the Ag particles react with H<sub>2</sub>O<sub>2</sub> to form AgOOH [30]. Then AgOOH reacts with the OH· radical (the decomposition of H<sub>2</sub>O<sub>2</sub>) to form the Ag-peroxo radicals species [31]. This radical interacts with C=C double bond of the cyclohexene to form a new organic intermediate. Finally, the OH· radical terminates the reaction and forms the cyclohexene epoxide. AgOOH is recovered and thus the catalytic cycle could be maintained [32] and cyclohexene epoxide is the major product of cyclohexene oxidation. On the other hand, oxidation proceeds when H<sub>2</sub>O<sub>2</sub> is activated on

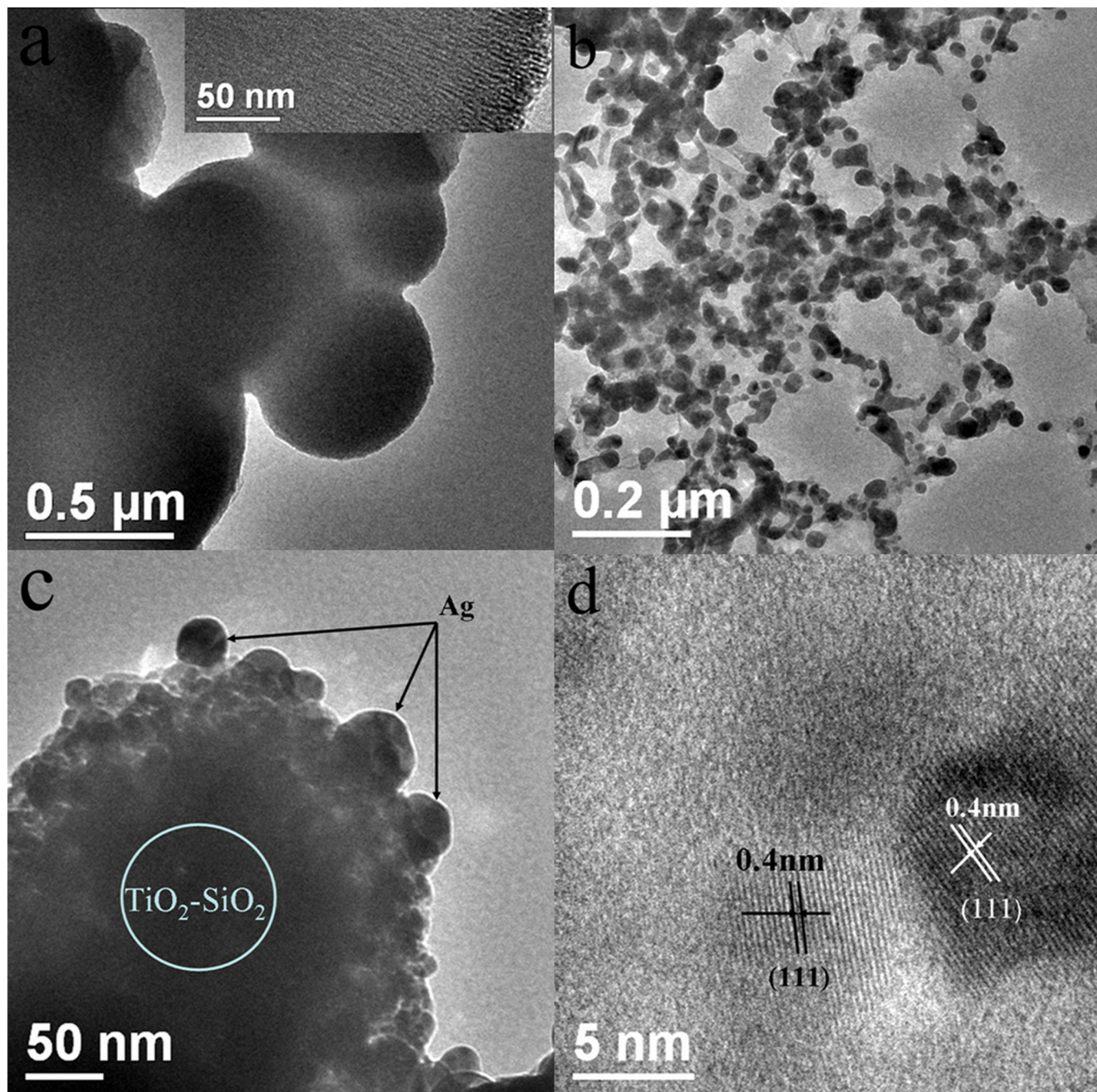


**Fig 4.** TEM images after calcination at 723 K of (a) TiO<sub>2</sub>-SiO<sub>2</sub>, (b) Ag (c) Ag-TS and (d)HRTEM image of Ag-TS.

<https://doi.org/10.1371/journal.pone.0176332.g004>

adjacent Ag sites, whereas hydrolysis to cyclohexanol occurs in the case that H<sub>2</sub>O adsorb on acidic OH· radical. From the fact that the former dominated the latter, even in the reaction with 30 wt % H<sub>2</sub>O<sub>2</sub> aqueous solution, the activation of H<sub>2</sub>O<sub>2</sub> is regarded as more frequent than H<sub>2</sub>O, and the activated peroxy species are more reactive than H<sub>3</sub>O<sup>+</sup> species. In this mechanism, the absence of detection of cyclohexene oxide is attributed to the rapid hydrolysis catalyzed by acidic OH· radical, too.

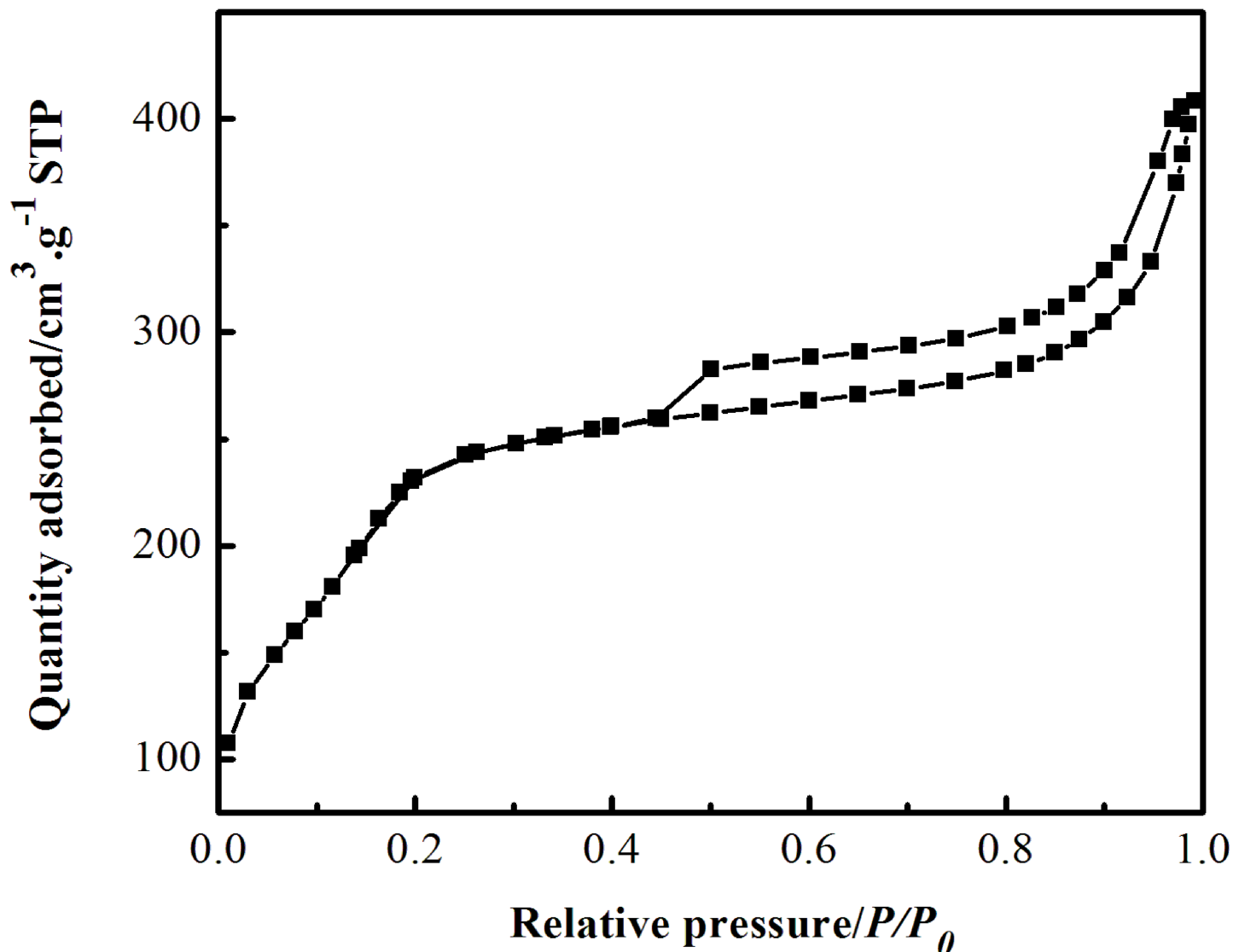
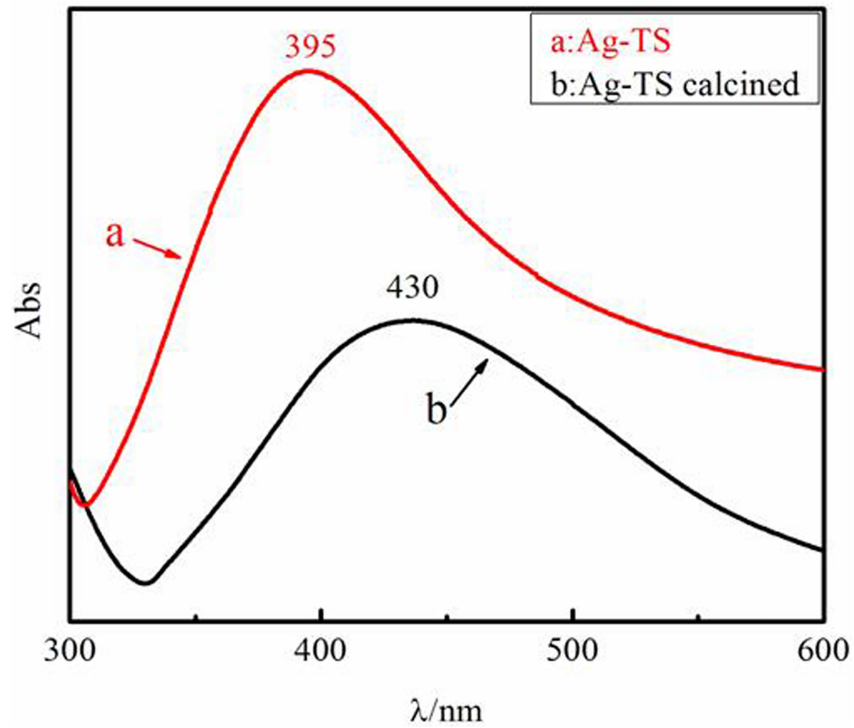


Fig 5. N<sub>2</sub> adsorption-desorption isotherms of Ag-TS at 77 K.

<https://doi.org/10.1371/journal.pone.0176332.g005>

Fig 9 shows the effect of temperature on epoxidation reaction is investigated from 298 to 353 K. At 298 K, low conversion rate is achieved by the Ag-TS catalyst. With an increase in the reaction temperature, the cyclohexene conversion increases from 39.2 to 99.2% and then decreases obviously to 45.7% at 373 K. When the reaction temperature is over 353 K, the selectivity to cyclohexene oxide drops dramatically. It is clearly that increasing the reaction temperature can quicken the reaction rate, but the higher reaction temperature can accelerate the decomposition of H<sub>2</sub>O<sub>2</sub>. The oxidant is decomposed by high temperature before oxidation, resulting in the decrease in the cyclohexene conversion and the selectivity to cyclohexene oxide. The results in Fig 9 show that the heating process is necessary for the epoxidation of cyclohexene over Ag-TS catalyst, but this temperature is not too high. Thus, based on the obtained results, the optimum catalytic condition (best conversion and selectivity to cyclohexene oxide) is at 353 K.





**Fig 6.** UV-Vis spectra of (a) Ag-TS particles; (b) Ag-TS particles after calcination at 723 K.

<https://doi.org/10.1371/journal.pone.0176332.g006>

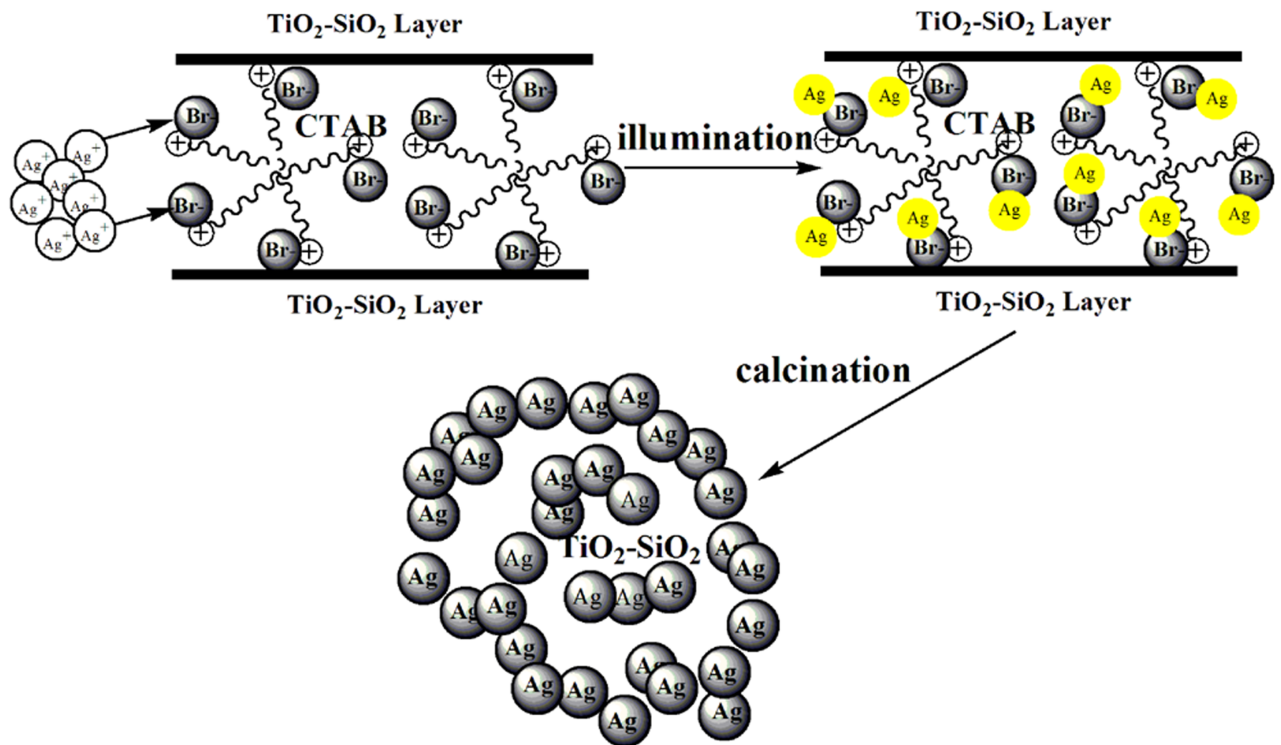


**Fig 7.** Formation mechanism of the Ag-TS composite.

<https://doi.org/10.1371/journal.pone.0176332.g007>

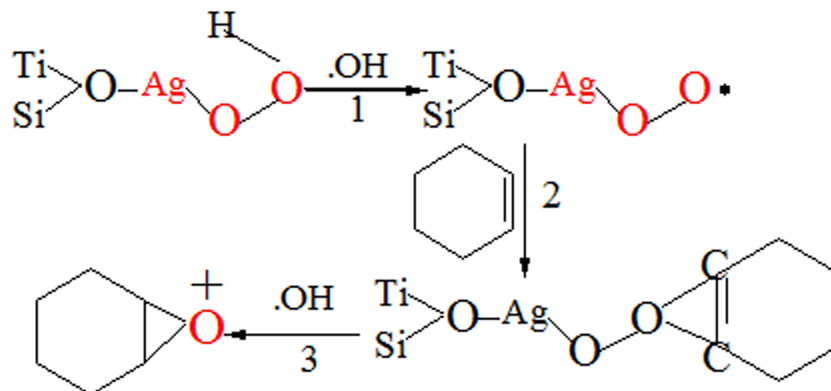


Fig 8. Plausible mechanism of epoxidation reaction.

<https://doi.org/10.1371/journal.pone.0176332.g008>

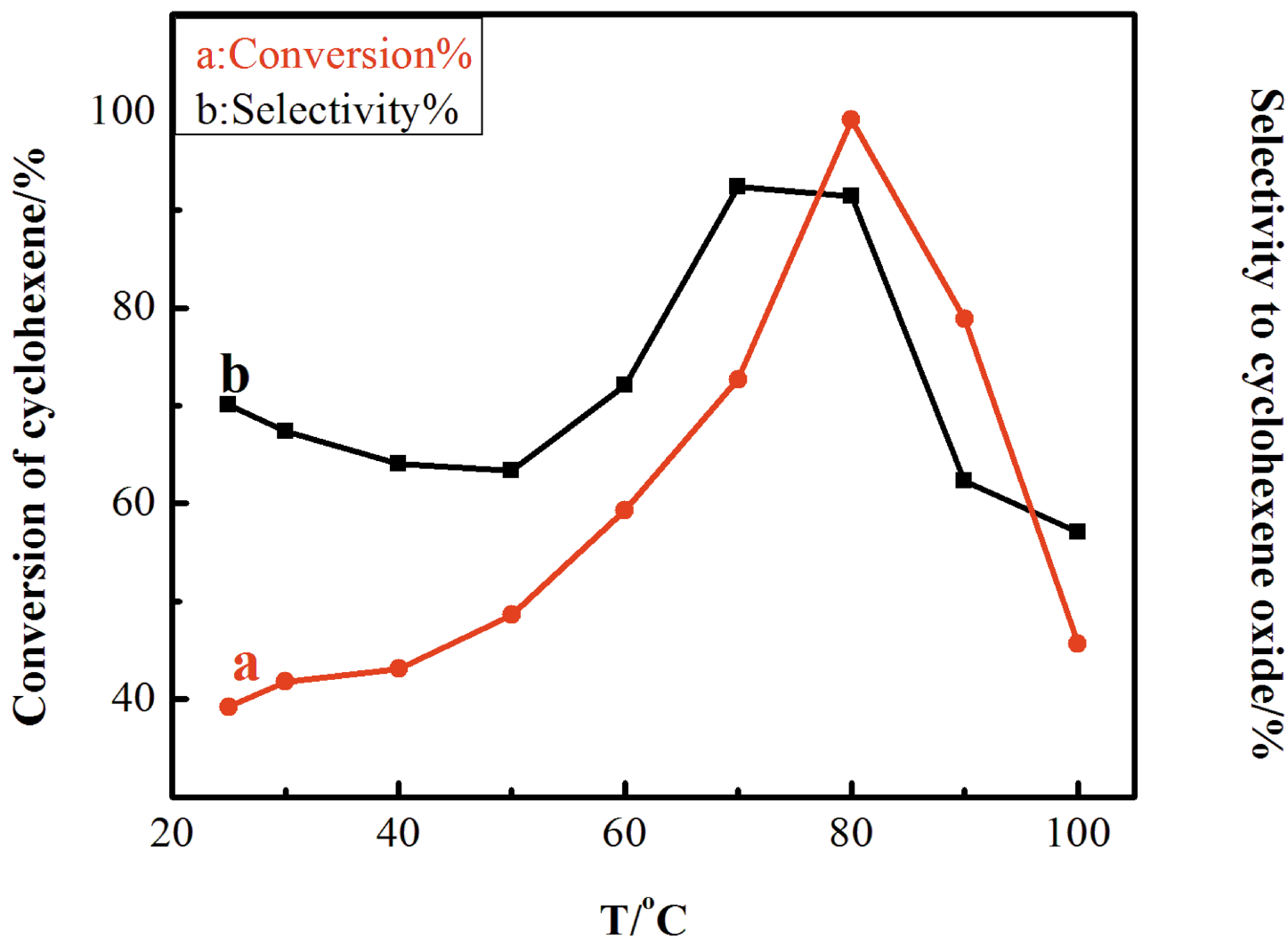
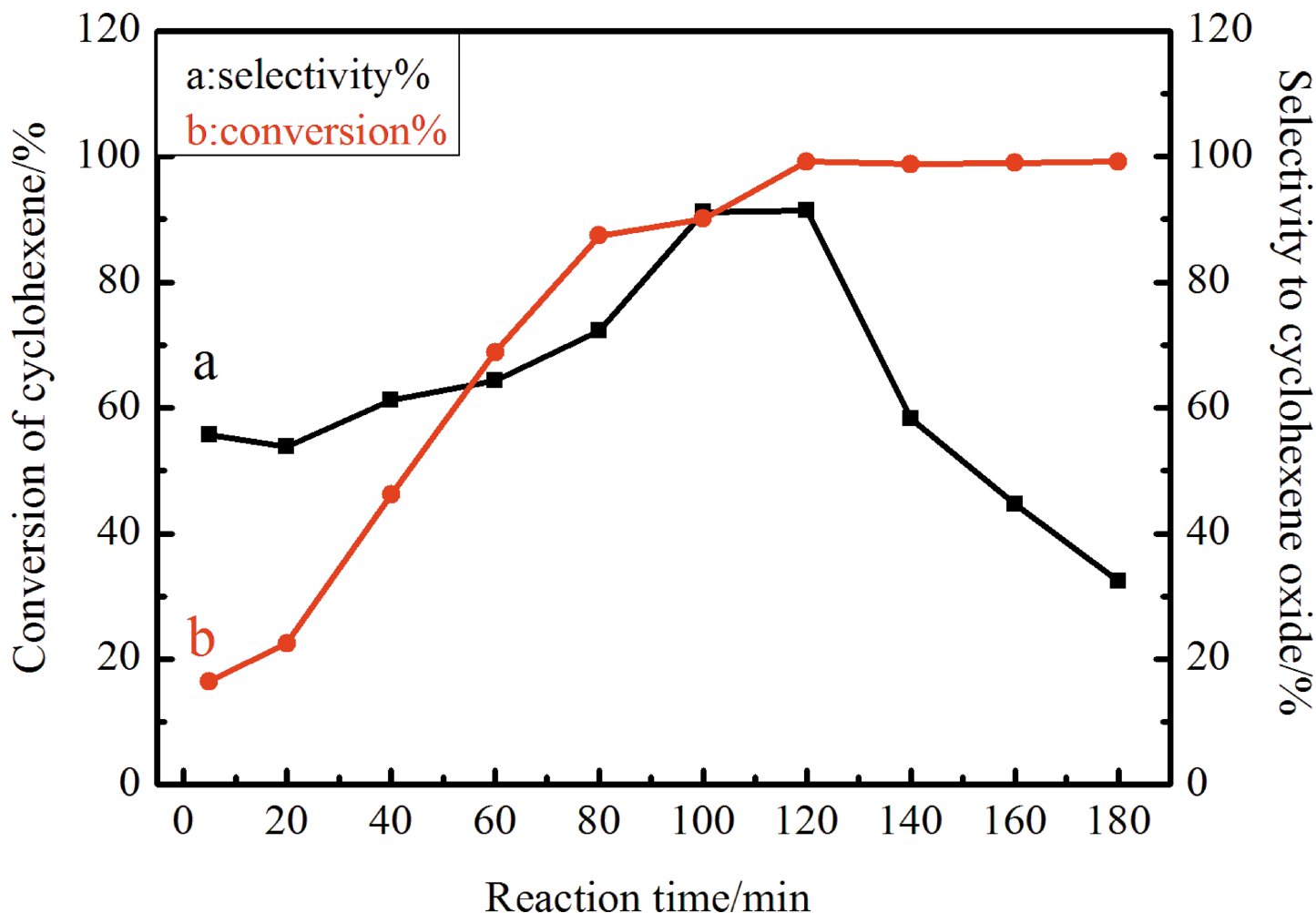


Fig 9. Effect of reaction temperature on the catalytic performance of Ag-TiO<sub>2</sub>-SiO<sub>2</sub> in the epoxidation of cyclohexene. (Reaction conditions: catalyst, 80 mg; cyclohexene, 6 mL; H<sub>2</sub>O<sub>2</sub>, 6 mL; chloroform, 12 mL; for 120 min).

<https://doi.org/10.1371/journal.pone.0176332.g009>





**Fig 10.** Effect of reaction time on the catalytic performance of Ag-TiO<sub>2</sub>-SiO<sub>2</sub> in the epoxidation of cyclohexene. (Reaction conditions: catalyst, 80 mg; cyclohexene, 6 mL; H<sub>2</sub>O<sub>2</sub>, 6 mL; chloroform, 12 mL; at 353 K).

<https://doi.org/10.1371/journal.pone.0176332.g010>

The conversion of cyclohexene and the product selectivity are monitored every 20 min in order to find out the optimum reaction time. Fig 10 shows the effect of the reaction time on the catalytic performance of Ag-TS in the epoxidation of cyclohexene at 353 K. With an increase in the reaction time from 5 to 180 min, the cyclohexene conversion increases from 16.5 to 99.2%, and the selectivity to cyclohexene oxide increases to a maximum for 120 min and then decreases obviously. When the reaction time is over 120 min, the cyclohexene oxide selectivity decreased from 91.4% to 32.4%, which was probably due to the subsequent reactions of the products. The result in Fig 10 shows that the reaction time is too long to proceed successfully to the target product. So it is very important to control the reaction time and the optimum reaction time for our system was 120 min.

The cyclohexene epoxidation is carried out using the three catalysts as oxidant and chloroform as solvent at 353 K for 120 min in Fig 11. TiO<sub>2</sub>-SiO<sub>2</sub> particles show the poor catalytic ability. Using Ag as a catalyst, 70.2% cyclohexene oxide conversion is achieved, which indicates that Ag particles is able to oxidize cyclohexene. When Ag-TS composite are used as a catalyst, the higher conversion and selectivity of cyclohexene are obtained with the main product of cyclohexene oxide, 99.2% cyclohexene oxide conversion and 91.4% selectivity are achieved. It is observed

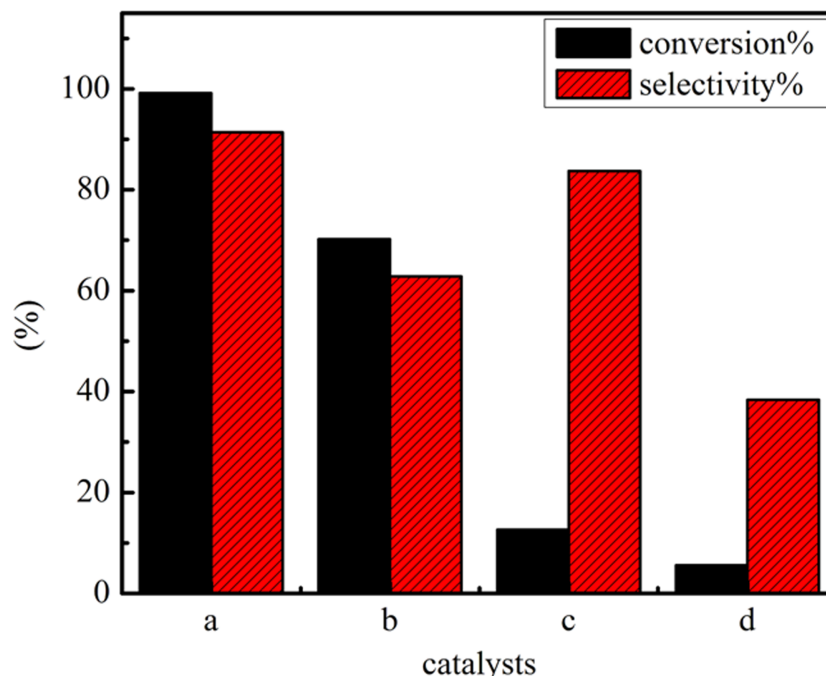


**Fig 11.** Effect on the catalytic performance of the three catalysts in the epoxidation of cyclohexene: (a) Ag-TiO<sub>2</sub>-SiO<sub>2</sub>; (b)Ag; (c) TiO<sub>2</sub>-SiO<sub>2</sub>; (d)blank (Reaction conditions: catalyst, 80 mg; cyclohexene, 6 mL; H<sub>2</sub>O<sub>2</sub>, 6 mL; chloroform, 12 mL; for 120 min).

<https://doi.org/10.1371/journal.pone.0176332.g011>

that the content of Ag in the catalysts played a crucial role in controlling the catalytic activity of the materials and the Ag species coated TiO<sub>2</sub>-SiO<sub>2</sub> have a higher catalytic activity for the epoxidation of cyclohexene. As a matrix of Ag particles, TiO<sub>2</sub>-SiO<sub>2</sub> particles possess higher activity for the epoxidation of cyclohexene and can provide more active sites for the adsorption of cyclohexene and therefore improve the cyclohexene conversion over Ag-TS catalyst. Our repeatable work is better than other similar researches [33–35], this demonstrates that TiO<sub>2</sub>-SiO<sub>2</sub> in Ag-TS has led to a synergetic action. The presence of the TiO<sub>2</sub>-SiO<sub>2</sub> composite oxide can enhance the reactants from contacting with the active sites using Ag-TS catalyst.

Table 1 shows the catalytic performance of Ag-TS composite calcined at different temperature for the epoxidation of cyclohexene. The results show that Ag-TS catalyst calcined at 723 K displays a higher cyclohexene epoxidation conversion and the most high epoxide yield. The

**Table 1.** Effect of Ag-TS particle after calcination at different temperature on the catalytic performance in the epoxidation of cyclohexene at 353 K.

Catalyst (calcination temperature)	conversion (%)	product selectivity(%)			
		cyclohexene oxide	cyclohexenone	cyclohexenol	others
blank test	0.82	38.5	20.1	43.1	trace
Ag-TS(298 K)	38.4	50.8	13.8	15.7	19.7
Ag-TS(523 K)	56.3	42.8	19.9	31.6	5.7
Ag-TS(623 K)	77.4	20.2	19.4	6.6	53.8
Ag-TS(723 K)	99.2	91.4	4.1	3.8	0.7
Ag-TS(823 K)	99.0	48.6	13.6	29.3	8.5
Ag-TS(923 K)	95.7	15.7	57.2	8.0	19.1

(Reaction conditions: catalyst, 80 mg; cyclohexene, 6 mL; H<sub>2</sub>O<sub>2</sub>, 6 mL; chloroform, 12 mL; for 120 min).

<https://doi.org/10.1371/journal.pone.0176332.t001>

conversion and selectivity of cyclohexene epoxidation are 99.2% and 91.4%, respectively. It is well-known that the transformation temperature of TiO<sub>2</sub> particles from the amorphousness to crystals is in the range of 573–873 K. TiO<sub>2</sub> of the TiO<sub>2</sub>-SiO<sub>2</sub> particles was near completely transformed to the anatase phase at 723 K, but amorphous SiO<sub>2</sub> were retained. The use of amorphous SiO<sub>2</sub> support for the dispersion of titanium oxide offers many advantages such as large specific surface area, high thermal stability, and good mechanical strength [36]. Ag particles would grow during the calcination temperature, which also cause the particles agglomeration and reduce catalyst activity. On the other hand, the presence of a second phase could effectively hinder such growth. It is found that the optimal calcination temperature for the Ag-TS composite is 723 K.

Being important chemical intermediates in the fine chemicals industry, cyclohexene oxide, cyclohexenone, cyclohexenol and others are usually produced of by the selective epoxidation of cyclohexene with H<sub>2</sub>O<sub>2</sub> as an oxidant. In the present research the epoxidation of cyclohexene is the primary product differs from the products of cyclohexene oxidization using other catalysts.

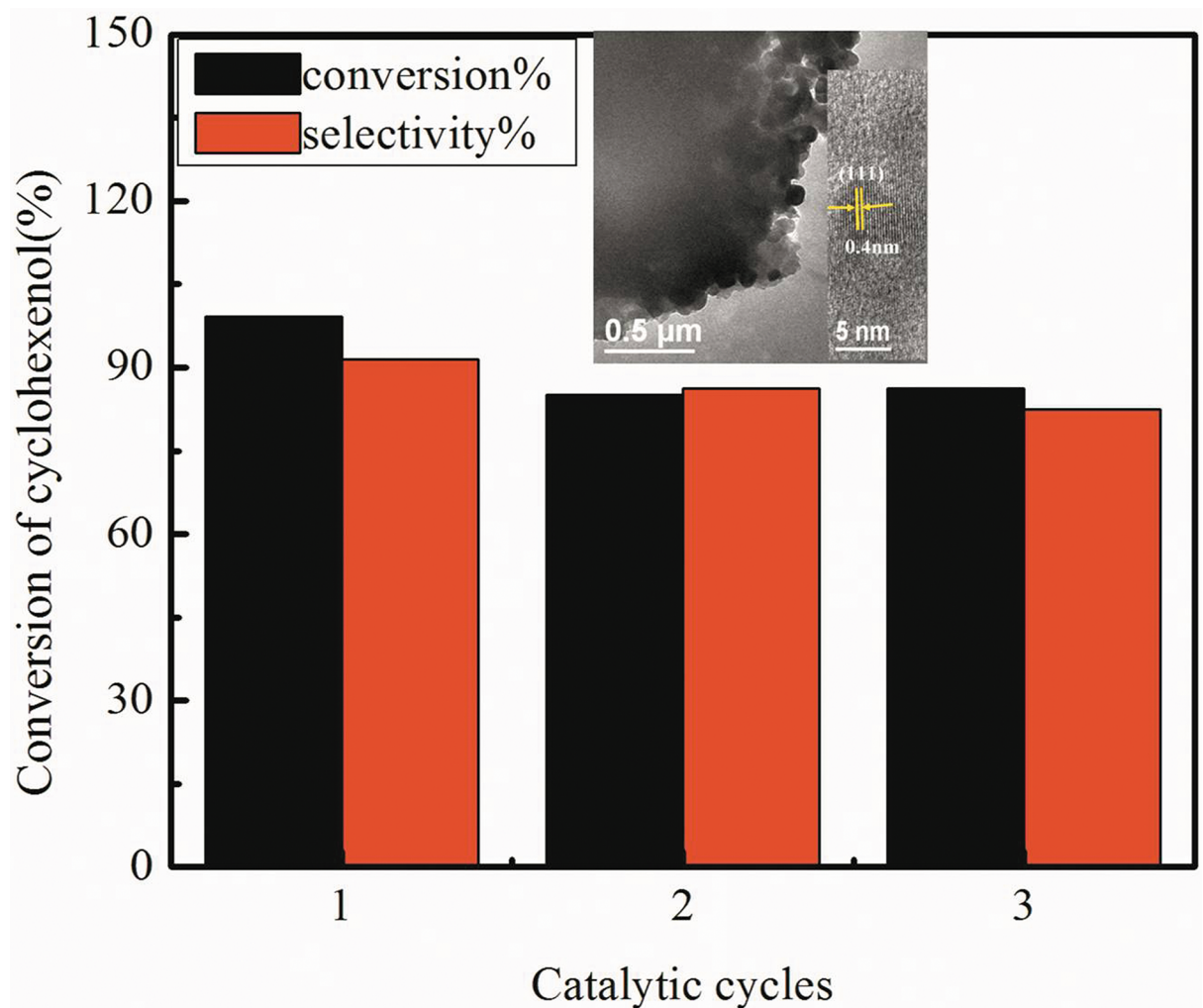


**Fig 12. Catalytic stability of Ag-TS catalyst, the inset is TEM images after catalytic reaction of Ag-TS catalyst.**

<https://doi.org/10.1371/journal.pone.0176332.g012>

## Catalyst stability

In order to examine the recyclability of the Ag-TS composite, the catalysts are recycled for three times to test their catalytic activities. After each cycle, the catalyst is recovered via centrifugation and washed with deionized water, dried at 353 K for 24 h and calcined in air at 723 K for 2 h. The reaction results show that the recovered Ag-TS catalyst after three recycles could maintain 83% of the initial catalytic activity (Fig 12). In the inset of Fig 12, the information about morphological structure of the synthesized catalyst after the catalytic reaction could be obtained by TEM. There was no significant change found in the morphology of catalyst. The HRTEM presents clear lattice fringe of the molecule packing, and the interlayer spacing is 0.4 nm which is corresponding to (111) facet of cubic crystal system.

## Conclusions

TiO<sub>2</sub>-SiO<sub>2</sub> particles are fabricated on air-water interface via self-assembling process and used as the substrate of Ag particles. The Ag-TS composites are successfully prepared by a soaking method without employing any reducing agent. Experimental results show that Ag particles are tightly loaded on the surface of TiO<sub>2</sub>-SiO<sub>2</sub>. XRD, SEM, EDS, BET, TEM and UV-Vis have been used to characterize morphologies and structures of the catalyst. The catalytic activity of Ag-TS composite after calcination for the cyclohexene epoxidization depend on the noble metal (Ag) loaded on the surface of TiO<sub>2</sub>-SiO<sub>2</sub>. The product calcined at 723 K has the best catalytic activity. The TiO<sub>2</sub>-SiO<sub>2</sub> particles possess synergistic catalytic activity. Using it as catalyst in cyclohexene oxidization reaction, the highest epoxide selectivity of 91.4% can be achieved. The reaction conditions, such as reaction time and reaction temperature have an obvious influence on the catalytic performance of Ag-TiO<sub>2</sub>-SiO<sub>2</sub>. In this experiment, the cyclohexene oxide is the major product. In addition, the activity of the Ag-TS catalyst remains nearly unchanged after three successive recycles of catalytic reactions. This indicates that the catalyst has a better stability of activity.

## Acknowledgments

Authors thank Ms Guoxu Qin for technical assistance.

## Author Contributions

**Conceptualization:** XW.

**Data curation:** XW XYW XHL.

**Formal analysis:** XW XHL.

**Funding acquisition:** XW.

**Investigation:** JYX XYW.

**Methodology:** XW JYX XYW.

**Project administration:** XW.

**Resources:** XW.

**Supervision:** XW.

**Validation:** JYX XHL.

**Visualization:** XW XHL.

**Writing – original draft:** XW.

**Writing – review & editing:** XW JYX XHL.

## References

1. Bradley CA, McMurdo MJ, Don Tilley T. Selective catalytic cyclohexene oxidation using titanium-functionalized silicone nanospheres. *J. Phys. Chem. C*. 2007; 111:17570–17579.
2. Cao YH, Yu H, Peng F, Wang HJ. Selective Allylic oxidation of cyclohexene catalyzed by nitrogen-doped carbon nanotubes. *Catal*. 2014; 3:1617–1625.
3. Qiu CJ, Zhang YC, Gao Y, Zhao JQ. Novel schiff-base complexes of methyltrioxorhenium (VII) and their performances in epoxidation of cyclohexene. *J. Organomet. Chem*. 2009; 694:3418–3424.
4. Behera GC, Parida KM. A comparative study of molybdenum promoted vanadium phosphate catalysts towards epoxidation of cyclohexene. *Appl. Catal. A: General*. 2013; 464–465: 364–373.
5. Muratsugu S, Weng Z, Tada M. Surface functionalization of supported Mn clusters to produce robust Mn catalysts for selective epoxidation. *Catal*. 2013; 3:2020–2030.
6. Moosavifar M, Arbat AN, Rezvani Z, Nejati K. Host (dealuminated Y zeolite)-guest (trinuclear metal clusters of Co, Mn and Cox/Mny) as nanocomposite catalysts for the epoxidation of cyclohexene. *J. Catal*. 2015; 36:1719–1725.
7. Rayati S, Sheybanifard Z, Amini MM, Aliakbari A. Manganese porphines-NH<sub>2</sub>@SBA-15 as heterogeneous catalytic systems with homogeneous behavior: Effect of length of linker in immobilized manganese porphine catalysts in oxidation of olefins. *J. Mol. Catal. A: Chem*. 2016; 423:105–113.
8. Chen JJ, Liu BF, Gao XH, Yan LF, Xu DG. Effects of heterogeneous-homogeneous interaction on the homogeneous ignition in hydrogen- fueled catalytic microreactors. *Int. J. Hydrogen Energy*. 2016; 41:11441–11454.
9. Doi Y, Haneda M, Ozawa M. Direct decomposition of NO on Ba catalysts supported on rare earth oxides. *J. Mol. Catal. A Chem*. 2014; 383–384: 70–76.
10. Yan YB, Jia XL, Yang YH. Palladium nanoparticles supported on CNT functionalized by rare-earth oxides for solvent-free aerobic oxidation of benzyl alcohol. *Catal. Today*. 2016; 259:292–302.
11. Tajbakhsh M, Alinezhad H, Nasrollahzadeh M, Kamali TA. Green synthesis of the Ag/HZSM-5 nanocomposite by using Euphorbia heterophylla leaf extract: A recoverable catalyst for reduction of organic dyes. *J. Alloys Compd*. 2016; 685:258–265.
12. Yang Q, Jones W, Wells PP, Morgan D, Dong LC, Hu BS, et al. Exploring the mechanisms of metal co-catalysts in photocatalytic reduction reactions: Is Ag a good candidate?. *Appl. Catal., A*. 2016; 518:213–220.
13. Liu S, Wu XD, Liu W, Chen WM, Ran R, Li M, et al. Soot oxidation over CeO<sub>2</sub> and Ag/CeO<sub>2</sub>: Factors determining the catalyst activity and stability during reaction. *J. Catal*. 2016; 337:188–198.
14. Hereijgers BPC, Parton RF, Weckhuysen BM. Cyclohexene epoxidation with cyclohexyl hydroperoxide: a catalytic route to largely increase oxygenate yield from cyclohexane oxidation. *Catal*. 2011; 1:1183–1192.
15. Tekla J, Tarach KA, Olejniczak Z, Girman V, Góra-Marek K. Effective hierarchization of TS-1 and its catalytic performance in cyclohexene epoxidation. *Microporous Mesoporous Mater*. 2016; 233:16–25.
16. Garcia AM, Moreno V, Delgado SX, Ramírez AE, Vargas LA, Vicente MÁ, et al. Encapsulation of SALEN- and SALHD-Mn(III) complexes in an Al-pillared clay for bicarbonate-assisted catalytic epoxidation of cyclohexene. *J. Mol. Catal. A: Chem*. 2016; 416:10–19.
17. Belaidi N, Bedrane S, Choukchou-Braham A, Bachir R. Novel vanadium- chromium-bentonite green catalysts for cyclohexene epoxidation. *Appl. Clay Sci*. 2015; 107:14–20.
18. Peng C, Lu XH, Ma XT, Shen Y, Wei CC, He J, et al. Highly efficient epoxidation of cyclohexene with aqueous H<sub>2</sub>O<sub>2</sub> over powdered anion-resin supported solid catalysts. *J. Mol. Catal. A: Chem*. 2016; 423:393–399.
19. Bet-Moushoul E, Farhadi K, Mansourpanah Y, Molaie R, Forough M, Nikbakht AM. Development of novel Ag/bauxite nanocomposite as a heterogeneous catalyst for biodiesel production. *Renewable Energy*. 2016; 92: 12–21.
20. Hosseini-Sarvari M, Ataee-Kachouei T, Moeini F. A novel and active catalyst Ag/ZnO for oxidant-free dehydrogenation of alcohols. *Mater. Res. Bull*. 2015; 72: 98–105.
21. Sun DL, Wang JJ, Yamada Y, Sato S. Cyclodehydration of diethylene glycol over Ag-modified Al<sub>2</sub>O<sub>3</sub> catalyst. *Appl. Catal. A*. 2015; 505:422–430.

22. Williams FJ, Bird DP, Palermo A, Santra AK, Lambert RM. Mechanism, selectivity promotion, and new ultra-selective pathways in Ag-catalyzed heterogeneous epoxidation. *J. Am. Chem. Soc.* 2004; 126:8509–8510. <https://doi.org/10.1021/ja039378y> PMID: 15238008
23. Liu JH, Wang F, Gu ZG, Xu XL. Styrene epoxidation over Ag-γ-ZrP catalyst prepared by ion-exchange. *Catal. Comm.* 2009; 10:868–871.
24. Al-Hardan NH, Abdul Hamid MA, Ahmed NM, Shamsudin R, Othman NK. Ag/ZnO/p-Si/Ag heterojunction and their optoelectronic characteristics under different UV wavelength illumination. *Sens. Actuators, A.* 2016; 242:50–57.
25. Sing KSW. Reporting physisorption data for gas/solid systems with special reference to the determination of surface area and porosity. *Pure&Appl. Chem.* 1982; 54: 2201–2218.
26. Mantri Y, Lippard SJ, Baik MH. Bifunctional binding of cisplatin to DNA: why does cisplatin form 1,2-intrastrand cross-links with Ag but not with GA?. *J. Am. Chem. Soc.* 2007; 129:5023–5024. <https://doi.org/10.1021/ja067631z> PMID: 17402732
27. Cao D, Jin XY, Gan L, Wang T, Chen ZL. Removal of phosphate using iron oxide nanoparticles synthesized by eucalyptus leaf extract in the presence of CTAB surfactant. *Chemosphere.* 2016; 159:23–31. <https://doi.org/10.1016/j.chemosphere.2016.05.080> PMID: 27268791
28. Bradley CA, McMurdo MJ, Don Tilley T. Selective catalytic cyclohexene oxidation using titanium-functionalized silicone nanospheres. *J. Phys. Chem. C.* 2007; 111:17570–17579.
29. Zhan WC, Guo YL, Wang YQ, Yun Guo, Liu XH, Wang YS, et al. Study of higher selectivity to styrene oxide in the epoxidation of styrene with hydrogen peroxide over La-doped MCM-48 Catalyst. *J. Phys. Chem. C.* 2009; 113:7181–7182.
30. Notari B. Microporous crystalline Titanium Silicates. *Adv. Catal.* 1996; 41:253–334.
31. Zhuang JQ, Yang G, Ma D, Lan XJ, Liu XM, Han XW, et al. In situ magnetic resonance investigation of styrene oxidation over TS-1 zeolites. *Angew. Chem. Int. Ed.* 2004; 43:6377–6380.
32. Wang AL, Yin HB, Ge C, Ren M, Liu YM, Jiang TS. Synthesis of hollow silver spheres using poly-(styrene-methyl acrylic acid) as templates in the presence of sodium polyacrylate. *Appl. Surf. Sci.* 2010; 256:2611–2613.
33. Reddy AS, Chen CY, Chen CC, Chien SH, Lin CJ, Lin KH, et al. Synthesis and characterization of Fe/CeO<sub>2</sub> catalysts: Epoxidation of cyclohexene. *J. Mol. Catal. A: Chem.* 2010; 318:60–67.
34. Kwon S, Schweitzer NM, Park S, Stair PC, Snurr RQ. A kinetic study of vapor-phase cyclohexene epoxidation by H<sub>2</sub>O<sub>2</sub> over mesoporous TS-1. *J. Catal.* 2015; 326:107–115.
35. He W, Fang Z, Tian QT, Shen WD, Guo K. Effective continuous flow Process for the epoxidation of cyclohexene. *Ind. Eng. Chem. Res.* 2016; 55:1373–1379.
36. Berube F, Nohair B, Kleitz F, Kaliaguine S. Controlled postgrafting of titanium chelates for improved synthesis of Ti-SBA-15 epoxidation catalysts. *Chem. Mater.* 2010; 22:1988–1992.